World Academy of Science, Engineering and Technology
International Journal of Medical and Health Sciences
Vol:1, No:6, 2007

A new muscle architecture model with non-uniform distribution of muscle fiber types

Javier Navallas, Armando Malanda, Luis Gila, Javier Rodríguez, and Ignacio Rodríguez

Abstract— **According to previous studies, some muscles present a non-homogeneous spatial distribution of its muscle fiber types and motor unit types. However, available muscle models only deal with muscles with homogeneous distributions. In this paper, a new architecture muscle model is proposed to permit the construction of non-uniform distributions of muscle fibers within the muscle cross section. The idea behind is the use of a motor unit placement algorithm that controls the spatial overlapping of the motor unit territories of each motor unit type. Results show the capabilities of the new algorithm to reproduce arbitrary muscle fiber type distributions.**

Index Terms— **muscle model, muscle architecture, motor unit, EMG simulation.**

I. Introduction

ELECTROMYIOGRAPHIC (EMG) modeling is an important tool widely used in research, as it helps to better understand the relationships between the neuromuscular organization and the electromyographic signals used for diagnosis in clinical neurophysiology routine. A typical EMG model comprises several parts, including muscle architecture, action potential, tissue effects, and electrode behavior.

There are only few available muscle architecture models in current literature. The existing models [1]–[3] deal with homogeneous muscles, intending to obtain simulated muscles where the motor units (MUs) are uniformly distributed over the muscle cross section (MCS), and the muscle fibers (MFs) belonging to the MUs, namely, the motor unit fibers (MUFs), are distributed with a constant density. However, those models have important limitations, including severe "edge effects" that cause MUs on the external parts of the MCS to have higher motor unit fiber densities (MUFDs), causing a mismatch between target MUFD and the actual MUFD of the algorithm outcomes [4]. By adapting an algorithm proposed by Schnetzer *et al.* [2], we showed in a previous paper that it is possible to eliminate the edge effect, obtaining a muscle architecture model that has homogeneous properties all over its MCS [5]. This way, undesirable non-uniformities are eliminated.

However, there are physiological evidences that point that the distribution of the MUs and MF types may not be uniform in certain muscles. Furthermore, there are evidences of steep changes in the distribution of the MF types across the MCS of certain muscles. A physiologically acceptable muscle model should be able to reproduce the different observed muscle architectures.

Manuscript received July 31, 2007.

J. Navallas (javier.navallas@unavarra.es), A. Malanda, J. Rodríguez and I. Rodríguez are with the Public University of Navarra.

L. Gila is with the Hospital of Navarra.

The aim of this paper is to introduce a modification of our previously presented model [5], in order to allow the simulation of muscles with non-uniform distribution of MF types. The degree of non-uniformity is controlled by a target function that must be predefined all over the MCS. This target function represents the probability of finding either a type I or a type II MF at a given point of the MCS.

The paper begins with a presentation of the physiological basis and findings that support the rationale of the proposed model. Afterwards, the algorithm defining the model is presented. Special attention is payed to the mechanism to fit the MU placement distribution so that the predefined spatial distribution of the MF-type probability is satisfied. Finally, the model is evaluated with different MF-type distributions and its capabilities and limitations are discussed.

II. The model

A. Physiological basis

The distribution of MU forces has been shown to be highly skewed [6]–[8], comprising much more low-force units than high-force ones. Fuglevand [9] modeled this distribution by means of an exponential function that relates the MU index and its maximum twitch force. Taking for granted that the number of MFs within a MU is the main factor affecting the twitch force variation [10]–[13], we can assume an exponential distribution for the number of fibers of the motor units, namely, the motor unit fiber number (MUFN). It is also observed a strong positive correlation between the MUFN and the motor unit territory (MUT) size [10], [12]–[15], that suggests a uniform value of the MUFD over the muscle cross-section (MCS) [12], [16], [17].

Enoka [17] gives the following example relating the MF-type distribution and MU-type distribution for the first dorsal interosseous (FDI): Feinstein [18] estimated the number of motoneurons of the FDI in 120, and the number of muscle fibers on 40,500, while Dennett and Fry [19] estimated the MF-type distribution on 50.3% type I, 44.7% type IIa, and 5% type IIb MFs; assuming the exponential model proposed by Fuglevand for the MU twitch force distribution, and a linear relationship between twitch force and MUFN, the MU type distribution results in 84% type I and 16% type II MUs. The same approach will be used in our model for the determination of the distribution of MU types; i.e., the proportion of MUs of each type, being the smallest ones of type I and the largest of type II.

All these previous studies do not take into account any consideration about spatial distribution. However, things may

be very complex even in architecturally simple muscles. In most species we can find regional variations in the distribution of fiber types within the muscle cross-section. Fiber types have been shown to vary, in different ways: from proximal (more glycolytic) to distal regions (more oxidative) [20]; from the superficial part of the fascicle (more fast-twitch) to the most deeper part of the fascicle (more slow-twitch) [21]; and from the superficial part of the whole muscle cross-section (more fast-twitch / type II) to the most deeper part of the muscle (more oxidative / type I) [22].

An extreme case is shown by Richmond *et al.* [23], in the obliquus capitis inferior muscle of a primate, where a step-like gradient of MF types from the superficial (type II) to the deep part (type I) is detected by means of ATPase histochemistry. Furthermore, Knight and Kamen [24] studied MU-type distributions by means of macro-EMG analysis and reported that superficial motor units are larger (type I MUs) than deeper motor units (type II) in human vastus lateralis, indicating a nonrandom localization of human MUs.

The presence of MF-type and MU-type non-uniform distributions has significant implications, both in clinical routine and in simulation studies. In clinical routine, unless such gradients are recognized and taken into account, they can introduce an unexpected bias in the collected data [24]. In simulation, since the validity of the results depends on the degree of accuracy of the model, synthetic EMG signals generated from models that do not account for these gradients do not faithfully represent of the muscle under study.

B. Model basis

The overlapping at a certain point $\vec{r}$, $s(\vec{r})$, is defined as the number of MUs covering this point for a given MU placement. That is, the overlapping is a random variable defined as

$$s(\vec{r}) = \sum_{i=1}^{N} s_i(\vec{r}) \tag{1}$$

where N is the number of MUs in the simulated muscle, and $s_i(\vec{r})$ stands for an indicator function, defined as

$$s_i(\vec{r}) = \begin{cases} 1 & \text{if } \vec{r} \in \Gamma_i \\ 0 & \text{if } \vec{r} \notin \Gamma_i \end{cases} \tag{2}$$

where Γ_i is the i-th MUT.

In terms of MU-types, since the MUs are sorted by its size, the overlapping can be expressed as the sum of the type I and type II overlapping, being:

$$s(\vec{r}) = s_I(\vec{r}) + s_{II}(\vec{r}) \tag{3}$$

Calling N_I to the number of type I MUs, we have that

$$s_I(\vec{r}) = \sum_{i=1}^{N_I} s_i(\vec{r}) \quad ; \quad s_{II}(\vec{r}) = \sum_{i=N_I+1}^{N} s_i(\vec{r}) \tag{4}$$

The key for an homogeneous distribution of the MF-types over the MCS is to place the MUs in such a disposition that the overlapping is almost constant all over the MCS, since a uniform overlapping implies that the innervation probability is also constant and equal for all the MUs [5]. This can be accomplished by the overlapping spatial variance minimization (OSVM) algorithm.

The i-th MU innervation probability, $P_{I_i}(\vec{r})$, is defined as the probability that the i-th MU innervates a MF placed at a point $\vec{r}$, given that the MF is actually covered by the i-th MU. As we demonstrated elsewhere [5], if the overall overlapping is almost constant across the MCS, and if the innervating MU is randomly selected from the set of covering MUs, the innervation probability is also almost constant and can be approximated by:

$$P_{I_i}(\vec{r}) \approx \overline{m_{P_I}} = \frac{1}{\overline{m_s}} \tag{5}$$

where $\overline{m_{P_I}}$ is the mean innervation probability, and $\overline{m_s}$ is the mean overlapping. The latter can be calculated as

$$\overline{m_s} = \frac{1}{A_{MCS}} \sum_{i=1}^{N} A_i \tag{6}$$

where A_{MCS} is the area of the MCS.

This approximation implies that the probability of a MF at $\vec{r}$ being innervated by a type I MU (hence, becomes a type I MF) is proportional to the overlapping of type I MUs at this point, since the total overlapping is constant across the MCS. That is:

$$P_{I_I}(\vec{r}) = \frac{s_I(\vec{r})}{s_I(\vec{r}) + s_{II}(\vec{r})} = \frac{s_I(\vec{r})}{\overline{m_s}} \tag{7}$$

where the equation

$$P_{I_I}(\vec{r}) + P_{I_{II}}(\vec{r}) = \frac{s_I(\vec{r})}{\overline{m_s}} + \frac{s_{II}(\vec{r})}{\overline{m_s}} = 1 \tag{8}$$

is clearly satisfied.

This is the key of our model: if the global overlapping is kept constant within the MCS, the overlapping proportion of each type of MUs determines the MF-type proportions, hence its probability. This allows us to transform the target MF-type distribution functions, $P_{I_I}^{target}(\vec{r})$ and $P_{I_{II}}^{target}(\vec{r})$, into target MU-type overlapping functions, $s_I^{target}(\vec{r})$ and $s_{II}^{target}(\vec{r})$ respectively, that we can use in our OSVM algorithm:

$$s_{II}^{target}(\vec{r}) = \overline{m_s}\ P_{I_{II}}^{target}(\vec{r}) \tag{9}$$

In the OSVM algorithm, a square grid of side a is placed over the MCS. This way, a set of K points (approximately $\pi(R/a)^2$) regularly spaced through the MCS is obtained. To adjust the overlapping of the type II MUs to the target function in (9), we can minimize the mean squared error of the overlapping over the set of points of the grid:

$$e_s = \frac{1}{K} \sum_{k=1}^{K} \left(s_{II}(\vec{q}_k) - s_{II}^{target}(\vec{q}_k) \right)^2 \tag{10}$$

Then, to place the type I MUs so that the global overlapping within the MCS is constant, we minimize the spatial variance of the global overlapping in the MCS. This can be estimated through the sample variance of the overlapping over the set of points of the grid:

$$v_s = \frac{1}{K} \sum_{k=1}^{K} \left(s(\vec{q}_k) - m_s \right)^2 \tag{11}$$

where m_s is the sample mean of the overlapping calculated as:

$$m_s = \frac{1}{K}\sum_{k=1}^{K} s(\vec{q}_k) \tag{12}$$

This way we ensure both a constant global overlapping, and a distribution of the MU types in accordance with a target distribution given by the target type II overlapping function.

C. Model algorithm

In the proposed model we make several physiological assumptions and approximations:

- The MCS is approximated by a circle of radius R.
- The MUTs are approximated by circles of radius R_i.
- The MFs are approximated by hexagons of apothem R_{MF}, placed over a regular grid.
- MUFD is assumed to be constant for all the MUs.
- MUFN is assumed to vary exponentially, satisfying the twitch-force Fuglevand law.
- The MUT area distribution is approximated by an exponential law.
- The N_I smaller MUs are assumed to be type I, and the rest (N_{II}) are assumed to be type II.
- The innervation of each MF is recreated as an equal probability competition among its covering MUs.

With these assumptions, the proposed model is described in the following algorithm:

1) Creation of the MCS as a circle of radius R.
2) Determination of the MUT radii applying the exponential law [1]:
$$R_i = \alpha \cdot exp(\beta \cdot i) \tag{13}$$
where α and β are calculated so that $R_1 = R_{min}$ and $R_N = R_{max}$.
3) Determination of the MUT positions, applying the OSVM algorithm as follows:
   a) Creation of the square spatial sampling grid, with side a.
   b) Determination of the number of type I MUs, N_I.
   c) Placement of the type II MUs in a random order. Each MUT is centered on the point of the grid that minimizes the sampling error in (10). If various points lead to the same minimum value, one of them is selected with equal probability. If the MUT centered in the selected position exceeds the MCS boundary, the value of its radius is recalculated so that the area of the MUT inside the MCS equals πR_i^2.
   d) Placement of the type I MUs in a random order. Each MUT is centered on the point of the grid that minimizes the sampling variance in (11). If various points lead to the same minimum value, or if the MUT centered in the selected position exceeds the MCS boundary, the solutions of the previous point are applied.
4) Creation of the hexagonal grid of MFs, with apothem R_{MF}, including only the MFs with its center inside the MCS.
5) Determination of the MU that innervates each MF, by equal probability random selection from all the MUs covering the MF.

The determination of the number of type I MUs, N_I, is done by calculating the expected number of type I MFs, M_I, from the target of the innervation for the type I MFs, and the expected number of MFs for the different MUs, modeled by the exponential function in (13), so that N_I is the minimum number of MUs needed to sum up M_I MFs [17].

D. Model evaluation

Simulations were performed in the Matlab™ 7 environment (The Mathworks, Natick, MA, USA). Critical parts of the code were written in C to accommodate the intensive computing requirements of the simulations. The default settings for our simulations correspond to the first dorsal interosseous muscle [17], [18], [25], a small muscle of the hand typically used in simulations of complete muscles. Unless explicitly stated, the input parameters for the simulations used throughout the paper are: $R = 7mm, N = 120, R_{min} = 1mm, R_{max} = 5mm, R_{fibre} = 55\mu m$, and $a = 0.35mm$.

The model was evaluated with four different MF-type distributions:

- Logistic sigmoid on distance:
$$P_{I_I}^{target}(\vec{r}) = (1 + exp(10.4 - 2d(\vec{r})))^{-1} \tag{14}$$
where $d(\vec{r})$ is calculated as
$$d(\vec{r}) = \sqrt{(r_x + 4)^2 + r_y^2} \tag{15}$$
and $\vec{r}$ is split into its two Cartesian coordinates (r_x, r_y).
- Complementary logistic sigmoid on distance:
$$P_{I_I}^{target}(\vec{r}) = 1 - (1 + exp(10.4 - 2d(\vec{r})))^{-1} \tag{16}$$
where $d(\vec{r})$ is calculated as previously.
- Step function on the x-axis:
$$P_{I_I}^{target}(\vec{r}) = \begin{cases} 1 & \text{if } r_x \leq 0 \\ 0 & \text{if } r_x > 0 \end{cases} \tag{17}$$
- Linear function on the x-axis:
$$P_{I_I}^{target}(\vec{r}) = (r_x - R)/2R \tag{18}$$

The four proposed functions have a mean value of 0.5 when integrated over the MCS, which means that the expected number of MFs of both types is the same; i.e., half of the total number of MF within the MCS, $M/2$. Although the first function resembles the MF-type distribution observed by Richmond *et al.* [23], it is important to note that these functions are proposed only for evaluation purposes, and that any particular implementation to simulate a given muscle should be preceded by an histochemical study to estimate the corresponding $P_{I_I}(\vec{r})$.

In Fig. 1, we can observe the simulation results obtained for the first MF-type spatial distribution function, with expectations and variances calculated over 10,000 different realizations of the muscle. In Fig. 1(a), we see that the expectation of the overlapping is almost constant, as pretended by the use of

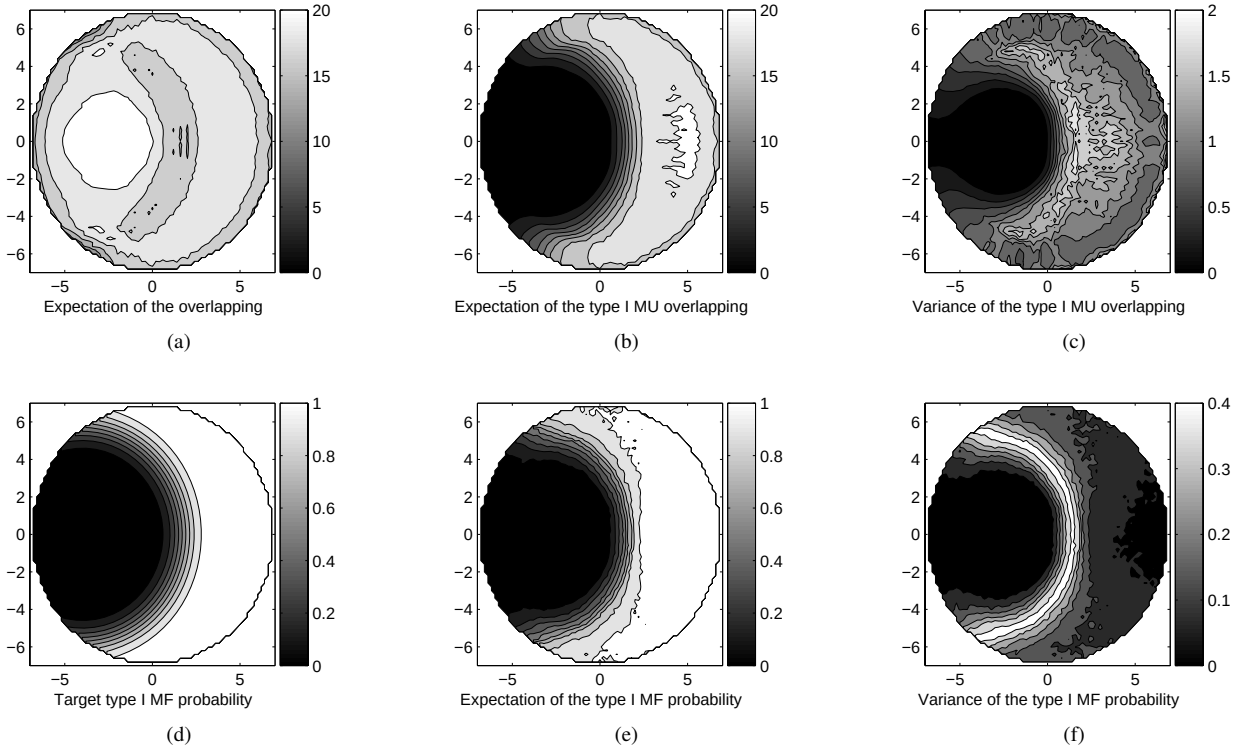

Fig. 1. Simulation results for the logistic sigmoid on distance MF-type spatial distribution given in (14) showing: (a) expectation of the global overlapping, $E[s(\vec{r})]$; (b) expectation of the type I MUs overlapping, $E[s_I(\vec{r})]$; (c) variance of the type I MUs overlapping, $Var[s(\vec{r})]$; (d) target type I MF probability spatial distribution, $P_{I_I}^{target}(\vec{r})$; (e) expectation of the type I MF innervation probability, $E[P_{I_I}(\vec{r})]$; and variance of the type I MF innervation probability, $Var[P_{I_I}(\vec{r})]$. The range of values of all the contour plots is shown on the right of each plot, and is divided in 10 equally spaced bins.

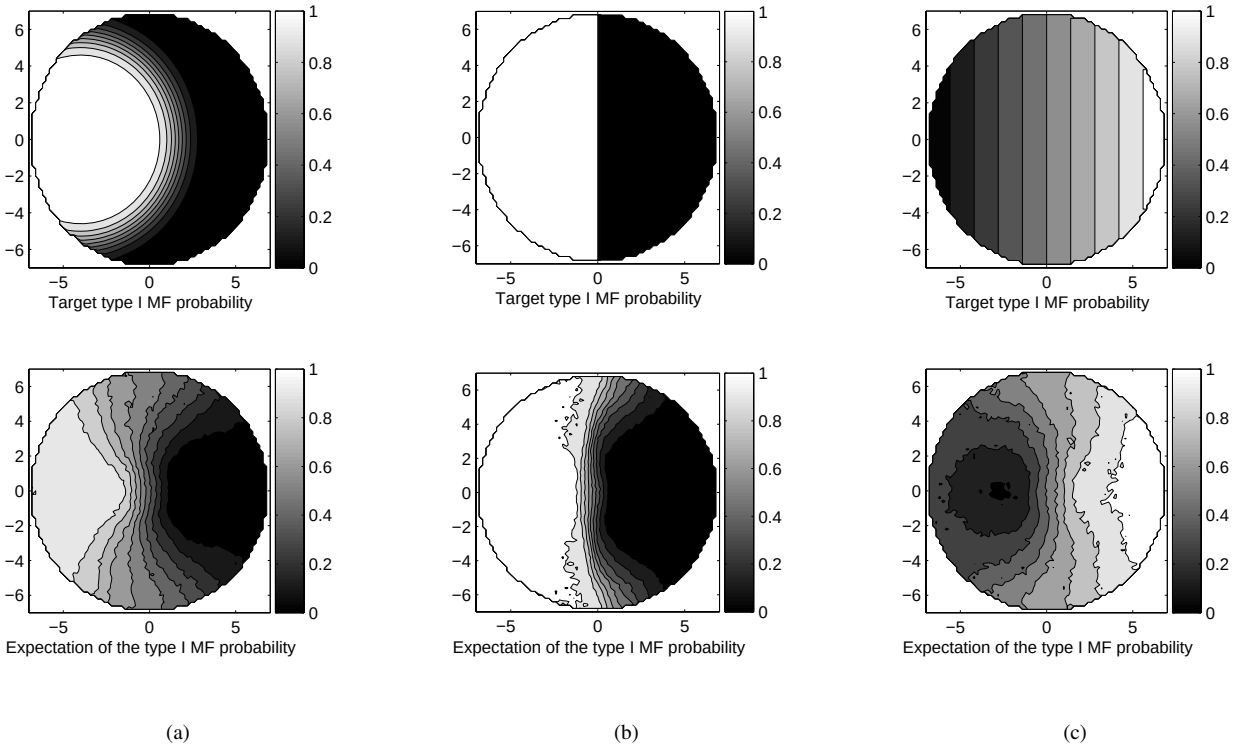

Fig. 2. Simulation results for three different MF-type spatial distributions: (a) complementary logistic sigmoid distribution as given in (16); (b) step function as given in (17); (d) linear function as given in (18). Each paired graph shows the target type I MF probability spatial distribution, $P_{I_I}^{target}(\vec{r})$ (upper plot) and the expectation of the type I MF innervation probability, $E[P_{I_I}(\vec{r})]$ (lower plot). The contour plots are divided into 10 equally spaced bins.

the OSVM algorithm. As we have seen, this is the prerequisite for the overlapping-innervation probability proportionality relationship given in (7) to be valid. This proportionality is experimentally proved when comparing the expectation of the MU-type overlapping in Fig. 1(b), with the expectation of the MF-type probability, in Fig. 1(e). In Fig. 1(c), we see the variance of the MU-type overlapping. We can see that the low variance properties of the OSVM are also present in the MU-type overlapping, in the modified algorithm. In the case of this logistic sigmoid target function, which is depicted in Fig. 1(d), we observe a high degree of matching between the target and the resulting MF-type distribution in Fig. 1(e). Finally, we can observe that the variance of the MF-type probability, shown in 1(f), is almost negligible in the areas where we find only one MF-type, while it increases in the transition regions, as expected where the MF-type proportions reach the 50%.

The evaluation with the other three patterns helps to understand the limitations of the algorithm to satisfy an arbitrary overlapping target function. It is important to remember that the pattern has to be reproduced by placing the MUT circles within the MCS in the most adequate positions, and that the MUT radii used in the simulations range from 1 to 5 mm, while the MCS has a radius of only 7 mm. In addition, when the MUT exceeds the MCS boundary, its radius is increased to satisfy the design value for the MUT area. This way, if a complex target function has to be reproduced, it is easier for the algorithm to reproduce the details with small MUs.

This can be observed in Fig. 2(a), where the complementary target function of that employed in Fig. 1 is used. Here, the detail of the "horns" must be covered by type II MUs, which are much bigger than type I MUs. Hence, the capability of reproducing this pattern is rather limited. In the case of a step function, as can be observed in Fig. 2(b), the steep gradient can be quite acceptably reproduced, with only some residual deficiencies that are present in the external parts of the MCS. Finally, when assuming a linear pattern, as in Fig. 2(c), the resulting MF-type distribution has a more progressive gradient, but also suffers from the difficulties derived from the large size of the type II MUs, as can be observed in the left part of the MCS, where the concentration of type I MUs was supposed to decrease as we move to the $(-R, 0)$ point, but it unexpectedly takes its maximum in a more inner region.

It has to be clear that smaller MUs will always lead to a better agreement between the target and the simulated MF-type distribution, but as in the case of the distribution itself, this should be grounded on experimental physiological data.

III. Conclusion

We have presented a model for muscle architecture that allows a non-uniform distribution of the MU types, and accordingly a non-uniform distribution of the MFs within the MCS. This is the first muscle architecture model that does not suppose an homogeneous distribution of MUs and MFs. This will allow for the simulation of muscles with higher degree of realism, and EMG signals with a better statistical agreement with those recorded in clinical routine.

References

[1] D. W. Stashuk, "Simulation of electromyographic signals," *J. Electromyogr. Kinesiol.*, vol. 3, pp. 157–173, 1993.
[2] M. A. Schnetzer, D. G. Ruegg, R. Baltensperger, and J. P. Gabriel, "Three-dimensional model of a muscle and simulation of its surface EMG," *Engineering in Medicine and Biology Society, 2001. Proceedings of the 23rd Annual International Conference of the IEEE*, vol. 2, pp. 1038–1043, 2001.
[3] A. Hamilton-Wright and D. W. Stashuk, "Physiologically based simulation of clinical EMG signals," *IEEE Trans. Biomed. Eng.*, vol. 52, pp. 171–183, 2005.
[4] J. Navallas, A. Malanda, L. Gila, J. Rodríguez, and I. Rodríguez, "Mathematical analysis of a muscle architecture model," *IEEE Trans. Biomed. Eng., submitted for publication.*
[5] ——, "New muscle architecture model with uniform motor unit fiber density," *IEEE Trans. Biomed. Eng., submitted for publication*.
[6] E. Henneman, G. Somjen, and D. O. Carpenter, "Functional significance of cell size in spinal motorneurons," *J. Neurophysiol.*, vol. 28, pp. 560–580, 1965.
[7] E. Henneman and C. B. Olson, "Relations between structure and function in the design of skeletal muscles," *J. Neurophysiol.*, vol. 28, pp. 581–598, 1965.
[8] H. S. Milner-Brown, R. B. Stein, and R. Yemm, "The orderly recruitment of human motor units during voluntary isometric contractions," *J. Physiol.*, vol. 230, pp. 359–370, 1973.
[9] A. J. Fuglevand, D. A. Winter, and A. E. Patla, "Models of recruitment and rate coding organization in motor-unit pools," *J. Neurophysiol.*, vol. 70, pp. 2470–2488, 1993.
[10] S. C. Bodine, R. R. Roy, E. Eldred, and V. R. Edgerton, "Maximal force as a function of anatomical features of motor unit in the cat tibialis anterior," *J. Neurophysiol.*, vol. 57, pp. 1730–1745, 1987.
[11] S. Chamberlain and D. M. Lewis, "Contractile characteristics and innervation ratio of rat soleus motor units," *J. Physiol.*, vol. 412, pp. 1–21, 1989.
[12] S. Bodine-Fowler, A. Garfinkel, R. R. Roy, and V. R. Edgerton, "Spatial distribution of muscle fibers within the territory of a motor unit," *Muscle Nerve*, vol. 13, pp. 1133–1145, 1990.
[13] K. Kanda and K. Hashizume, "Factors causing differences in force output among motor units in the cat medialis gastrocnemius muscle," *J. Physiol.*, vol. 448, pp. 677–695, 1992.
[14] S. C. Bodine, A. Garfinkel, R. R. Roy, and V. R. Edgerton, "Spatial distribution of motor unit fibers in the cat soleus and tibialis anterior muscles: local interactions," *J. Neurosci.*, vol. 8, pp. 2142–2152, 1988.
[15] R. R. Roy, A. Garfinkel, M. Ounjian, J. Payne, A. Hirahara, E. Hsu, and V. R. Edgerton, "Three-dimensional structure of cat tibialis anterior motor units," *Muscle Nerve*, vol. 18, pp. 1187–1195, 1995.
[16] R. L. Lieber and J. Fridén, "Functional and clinical significance of skeletal muscle architecture," *Muscle Nerve*, vol. 23, pp. 1647–1666, 2000.
[17] R. M. Enoka and A. J. Fuglevand, "Motor unit physiology: some unresolved issues," *Muscle Nerve*, vol. 24, pp. 4–17, 2001.
[18] B. Feinstein, B. Lindegard, E. Nyman, and G. Wohlfart, "Morphologic studies of motor units in normal human muscles," *Acta Anat*, vol. 23, pp. 127–142, 1955.
[19] X. Dennett and H. J. H. Fry, "Overuse syndrome: a muscle biopsy study," *Lancet*, pp. 905–908, 1988.
[20] G. C. Elder, K. Bradbury, and R. Roberts, "Variability of fiber type distributions within human muscles," *J. Appl. Physiol.*, vol. 53, pp. 1473–1480, 1982.
[21] S. Grotmol, G. K. Totland, H. Kryvi, A. Breistol, B. Essen-Gustavsson, and A. Lindholm, "Spatial distribution of fiber types within skeletal muscle fascicles from standardbred horses," *Anat. Rec.*, vol. 268, pp. 131–136, 2002.
[22] J. Lexell, K. Henriksson-Larsen, and M. Sjostrom, "Distribution of different fiber types in human skeletal muscles. 2. a study of cross-sections of the whole m. vastus lateralis," *Acta Physiol. Scand.*, vol. 117, pp. 115–122, 1983.
[23] F. J. R. Richmond, K. Singh, and B. D. Corneil, "Marked non-uniformity of fiber-type composition in the primate suboccipital muscle obliquus capitis inferior," *Exp. Brain Res.*, vol. 125, pp. 14–18, 1999.
[24] C. A. Knight and G. Kamen, "Superficial motor units are larger than deeper motor units in human vastus lateralis muscle," *Muscle Nerve*, vol. 31, pp. 475–480, 2005.
[25] R. D. Adams and J. D. Reuck, "Metrics of muscle," in *Basic Research in Miology. Proceedings of the Second International Congress on Muscle Diseases*, B. A. Kakulas, Ed., 1971, pp. 3–11.